Computer Science and Information Systems 22(1):311–325 https://doi.org/10.2298/CSIS241107010C

Linear Projection-Based Noise Filtering Framework for Image Denoising

Congyin Cao, Yangjun Deng, Menglong Yang, and Xinghui Zhu*

School of Information and Intelligence, Hunan Agricultural University,
Changsha 410128, China
19913809590@stu.hunau.edu.cn
dyj2012@yeah.net
y602367035@163.com
zhuxh@hunau.net

Abstract. Image denoising remains a fundamental challenge in digital image processing due to the inevitable presence of noise during image acquisition and transmission. While existing noise filtering methods predominantly focus on local spatial information, they often overlook crucial structural information from other perspectives, such as local manifold and global structures. To address this limitation, we propose a novel linear projection-based noise filtering (LPNF) framework grounded in linear projection learning theory. This framework innovatively learns a linear projection for noise filtering by incorporating multiple structural information sources - local spatial, local manifold, and global structures - through well-defined criteria. We present two specialized implementations of the LPNF framework: PCA-based LPNF (LPNF-PCA) and LPP-based LPNF (LPNF-LPP). The LPNF-PCA simultaneously leverages local spatial and global information, while LPNF-LPP integrates both local manifold and spatial information for enhanced denoising performance. Comprehensive experiments conducted on four standard test images with various noise types demonstrate that both LPNF-PCA and LPNF-LPP consistently outperform state-of-the-art denoising methods in terms of both quantitative.

Keywords: Image denoising, linear projection-based noise filtering framework, principle component analysis, locality preserving projection.

1. Introduction

In the era of rapid technological advancement, digital imaging has become increasingly prevalent across various domains. The surge in artificial intelligence research has positioned digital image processing as a critical focus in computer vision applications. Digital images play instrumental roles in diverse applications, ranging from face recognition and satellite television to computed tomography. However, the quality of these images is invariably compromised by various types of noise, primarily due to sensor material limitations and environmental interference during image acquisition and transmission. Common noise types affecting digital images include Gaussian noise, Salt-and-Pepper noise, Scattering noise, Poisson noise, and various combinations thereof [3,15,20,26]. Consequently, image denoising has emerged as both a fundamental challenge and an essential preprocessing step in image processing applications.

* Corresponding author

Image denoising methods can be broadly categorized into two fundamental approaches: spatial domain and frequency domain techniques [5,13]. Among these, spatial domain filtering methods have reached a higher level of theoretical maturity and practical application. Representative approaches in the spatial domain include Gaussian filtering, mean filtering, and non-local mean filtering [6,10], which form the foundation of modern denoising techniques. Recent advances in this domain have led to significant improvements in denoising performance. For instance, Gao et al. [2] developed an innovative Gaussian filtering approach utilizing random weighting, which addresses the limitations of traditional Gaussian filtering in nonlinear system state estimation through adaptive noise characteristic estimation. Zhang et al. [28] introduced a fast combined median and mean filtering method that effectively suppresses both impulse and Gaussian noise simultaneously, representing a significant advancement in multi-noise suppression. Further innovations include the adaptive switching weight mean filter (ASWMF) proposed by Thanh et al.[21], specifically designed for salt-and-pepper noise removal, and an enhanced adaptive median filtering method developed by Tang et al. [19] that overcomes the limitations of conventional median filtering techniques in structured light image denoising. Huang and Ji [8] proposed an image denoising method that combines diffusion probability and dictionary learning. The approach aims to improve edge clarity during noise removal, addressing issues where traditional methods may blur edge information. These spatial domain methods have demonstrated remarkable effectiveness in noise removal and have gained widespread adoption across various image processing applications.

In the frequency domain, digital filtering methods have evolved significantly since the introduction of Fourier transform-based techniques, with low-pass and high-pass filters serving as foundational approaches [18]. Recent years have witnessed substantial advancements in frequency domain filtering algorithms. For instance, Zhang et al. [27] enhanced the optimal computation of center weight by incorporating a Wiener filter into the calculation process, achieving superior denoising results compared to traditional nonlocal mean methods. A notable contribution by Liu et al. [12] introduced the parallelizable Fast Multi-channel Wiener Filter (FMWF) algorithm, representing a significant advancement in computational efficiency. In addressing the specific challenges of hyperspectral imaging, Aswathy et al. [1] developed an innovative sparsity-based denoising strategy that effectively processes each band of hyperspectral images (HSI), demonstrating particular efficacy in this specialized domain. Further expanding the theoretical framework, Selesnick et al. [17] proposed an integrated approach combining low-pass filtering with total variation modeling, establishing a more comprehensive basis for frequency domain denoising.Yang and Li [25] proposed a method that enhances wavelet domain features to improve noisy image segmentation,the techniques discussed could be relevant to noise filtering applications.

Despite the advances in existing noise filtering methods, a significant limitation persists: these approaches typically consider image data from a single perspective, overlooking valuable information from other structural aspects. To address this limitation, we propose a novel linear projection-based noise filtering (LPNF) framework, grounded in projection learning theory. This framework innovatively integrates multiple structural aspects - local spatial information, local manifold structure, and global structure - through well-defined criteria to learn an optimal linear projection for noise filtering.

The proposed LPNF framework demonstrates remarkable flexibility, as it can accommodate various projection learning criteria commonly used in feature extraction for denoising purposes. We present two specific implementations of this framework: Principal Component Analysis-based LPNF (LPNF-PCA) and Locality Preserving Projection-based LPNF (LPNF-LPP). These implementations leverage the established criteria of PCA and LPP, respectively, to learn effective linear projections for noise filtering. Notably, LPNF-PCA achieves simultaneous consideration of both local spatial and global information, while LPNF-LPP effectively preserves the local manifold structure while maintaining spatial information integrity.

To rigorously evaluate the effectiveness of our proposed framework, we conduct comprehensive experiments on four standard test images corrupted with various types of noise. These experiments are designed to assess both the quantitative performance and visual quality of the denoising results.

2. Related Works

2.1. Principal Component Analysis

Principal Component Analysis (PCA) is a widely used dimensionality reduction technique in data science and machine learning, introduced by Pearson [14] and later formalized by Hotelling [7]. It transforms a dataset into a new coordinate system, where the axes (principal components) represent directions of maximum variance. PCA is particularly effective for simplifying data, reducing redundancy, and visualizing high-dimensional datasets. PCA works by computing the eigenvalues and eigenvectors of the covariance matrix of the data, where the eigenvectors define the principal components, and the eigenvalues represent the variance captured by each component. By retaining components with the largest eigenvalues, PCA minimizes information loss while reducing dimensionality. This property makes it valuable in fields like image compression, facial recognition, and gene expression analysis [11]. A key strength of PCA lies in its unsupervised nature and computational efficiency. However, it assumes linear relationships in the data, limiting its effectiveness for datasets with nonlinear structures. Variants like Kernel PCA address this limitation by mapping data into higher-dimensional feature spaces [16].

Despite its simplicity, PCA remains foundational in data analysis. Its applications extend across disciplines, including computer vision, finance, and biology, offering insights by emphasizing the most significant patterns in complex datasets.Principal Component Analysis (PCA) is a fundamental unsupervised dimensionality reduction and feature extraction technique that has garnered significant attention across various domains of data analysis and machine learning. The core principle of PCA is to transform high-dimensional data into a lower-dimensional subspace while maximizing variance and minimizing the correlation between features [23].

Mathematically, given an observation data matrix $[x_i] \in R^{(d\times n)}$, where $x_i \in R^d$ represents individual data points, d denotes the feature dimension, and n indicates the number of samples, PCA aims to find an optimal projection matrix P that minimizes the reconstruction error [24]. This optimization problem can be formally expressed as:

$$\min_{P} \sum_{i=1}^{n} \left\| x_i - PP^T x_i \right\|_2^2 \quad s.t. P^T P = I. \tag{1}$$

2.2. Classical Image Noise Filtering Methods

Classical image noise filtering methods include mean filter, bilateral filter, and median filter, etc. These are foundational techniques in image denoising, widely used for their simplicity and effectiveness in reducing noise while preserving image quality to varying degrees.The mean filter is a linear smoothing technique that replaces each pixel with the average value of its surrounding pixels. This method effectively reduces random noise but often blurs edges and fine details, making it less suitable for images where edge preservation is critical [4].The bilateral filter, introduced by Tomasi and Manduchi [22], is a nonlinear method that combines spatial proximity and pixel intensity differences to preserve edges while removing noise. By weighting nearby pixels based on both their spatial distance and intensity similarity, the bilateral filter avoids the over-smoothing associated with linear filters and is especially effective for images with fine textures.The median filter is another nonlinear approach, replacing each pixel with the median value of its neighborhood. This method excels in removing impulse noise (e.g., salt-and-pepper noise) without blurring edges, making it ideal for applications requiring robust noise suppression and edge preservation [9].In general, those methods can be summarized in a common framework as presented in Algorithm 1.

Problem Formulation: Given:

Input noisy image $Q = [q_{ij}] \in R^{a \times b}$

where a and b represent image dimensions $k \times k$ denotes the size of sliding window.

Objective:

Generate denoised image $Q' = [q_{ij}]$ through spatial convolution operations General Framework:

Window Operation:

For each pixel q_{ij} in Q

Apply $k \times k$ sliding spatial window

Generate local patch $I_{ij} \in R^{k \times k}$

Filtering Process:

Compute weight matrix W_{ij} specific to each method

Perform convolution: $q'_{ij} = W_{ij} * I_{ij}$

where * denotes convolution operation.

Specifically, in Algorithm 1, the different definitions of weight matrix W_{ij} represent different noise filters. For example, the mean filter is related the weight matrix whose elements are all equal to $\frac{1}{k2}$. The formula for constructing the weight matrix of the bilateral filter is:

$$W_{ij} = \omega s \times \omega r \tag{2}$$

where $\omega s = e^{\left(-\frac{(i-k)^2+(j-l)^2}{2\sigma_s^2}\right)}$ is the spatial distance factor and $\omega r = e^{\left(-\frac{\|I_{ij}-I_{kl}\|^2}{2\sigma_r^2}\right)}$ is the difference factor of grayscale. σ_s and σ_r are the filter parameters.

Algorithm 1: Classical noise filtering methods
Input: Noisy image $Q = [q_{ij}] \in R_{a\times b}$
for $i \leq a$ do
  for $j \leq b$ do
  Step 1: Generate a local patch $I_{ij} \in R^{k\times k}$ around each pixel q_{ij}
  with a $k \times k$ sliding spatial window.
  Step 2: For each patch I_{ij}, compute a corresponding weight matrix $W_{ij} \in R^{k\times k}$.
  Step 3: Convolution operation on pixel q_{ij} to get denoised pixel
  $q'_{ij} = W_{ij} * I_{ij}$, where * is a convolution operation.
  end
end
Step 4: Restore the denoised image $Q' = \left[q'_{ij}\right] \in R^{a\times b}$.
Output: Denoised image Q'

3. Methodology

3.1. Linear Projection-Based Noise Filtering Framework

Digital image acquisition and transmission processes are inherently susceptible to various types of noise, stemming from both imaging equipment limitations and environmental interference. These noise artifacts significantly degrade image quality, making image denoising a crucial preprocessing step in numerous computer vision applications. While traditional image filtering approaches employ sliding window-based convolution operations for noise reduction, they primarily focus on local spatial information, overlooking other valuable structural characteristics such as local manifold relationships and global image patterns.

To address these limitations, we propose a novel Linear Projection Noise Filtering (LPNF) framework that approaches image denoising from a data transformation perspective using linear projection theory. This framework uniquely integrates multiple structural aspects of image data:

- Local spatial information for detail preservation
- Local manifold structure for neighborhood relationships
- Global structure for overall image coherence

The detailed architecture of our proposed LPNF framework, illustrated in Fig 1, demonstrates how these different information sources are systematically integrated to achieve superior denoising performance.

In particular, assume

$Q = [q_{ij}] \in R^{a\times b}$ is a nosiy image and the size of the sliding window is $k \times k$,the detailed procedure of the proposed LPNF contains four steps. Namely,

Step1. For each pixel q_{ij}, a sliding window with size of $k \times k$ is employed to generate a local patch $I_{ij} \in R^{k\times k}$ around the center pixel q_{ij}, where $0 < i \leq a$ and $0 < j \leq b$.

Step2. Obtain data matrix X by vectorizing each patch I_{ij} into a row vector x_n, where $n = i + (j-1) \times a$. The data matrix X contains the local spatial information of image.

Step3. Construct a certain criterion to compute a linear projection $P \in R^{m\times k^2}$, $\left(m < k^2\right)$ for noise filtering.

Step4. Compute each noise filtered center pixel q'_{ij} by the following equation:

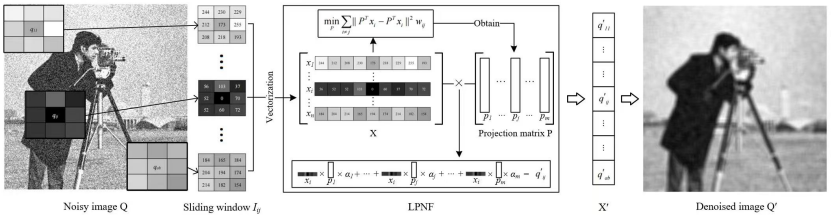

Fig. 1. The flowchart of LPNF framework

$$q'_{ij} = x_i * \sum_{j=1}^{m} p_j \alpha_j \tag{3}$$

where $p_j \in R^{k^2}$ is the column vector of linear projection P . Then, the denoised image Q' can be obtained by reorganizing the transformed data into a matrix of $a \times b$.

3.2. The Computation of Projection Matrix P

In our proposed LPNF framework, the selection and formulation of projection learning criteria play a pivotal role in determining denoising performance. The framework's flexibility allows for the incorporation of various projection learning approaches, particularly those developed within the graph embedding paradigm. Drawing from extensive literature review, we can formulate a generalized objective function for projection learning as follows:

$$\begin{aligned} \tilde{P} &= arg \min_{P^T X L_p X^T P} \sum_{i \neq j} \left\| P^T x_i - P^T x_j \right\|^2 \omega_{ij} \\ &= arg \min_{P^T X L_p X^T P} tr\left(P^T X L X^T P \right), \end{aligned} \tag{4}$$

where L is the Laplacian matrix of the intrinsic graph $G, L = D - W$, W is the graph weight matrix, D is a diagonal matrix with the ith diagonal element being $Dii = \sum_{j=1}^{n} w_{ij}$, and L_p may be the Laplacian matrix of the penalty graph G_p or a simple scale normalization constraint. By taking the structure information from different aspects into consideration, the weighted matrix W can be defined with different criteria.

The optimal solution of the minimizing problem (4) is equivalent to the generalized eigenvectors of the following generalized eigen-decomposition problem.

$$XLX^T p = \lambda X L_p X^T p \tag{5}$$

Thus, the optimal $\tilde{P}$ consists of the generalized eigenvectors corresponding to the m smallest nonzero eigenvalues of (5).

3.3. LPNF-PCA and LPNF-LPP

The objective function in our projection learning framework can be formulated using different criteria, primarily distinguished by their approaches to constructing the weight matrix W. We present two specialized implementations of LPNF, each representing a distinct methodology for capturing different aspects of image structure.

1) LPNF-PCA Implementation:

This first variant employs Principal Component Analysis (PCA) criteria for computing the linear projection. The weight matrix W is constructed as: $w_{ij} = 1/n$, for $j \neq i$

where:

- w_{ij} represents the $(i, j) - th$ element of matrix W
- n is the total number of samples
- The condition $j \neq i$ ensures proper handling of self-connections

This formulation enables LPNF-PCA to simultaneously capture:

- Local spatial relationships
- Global structural patterns
- Overall data distribution characteristics

2) LPNF-LPP Implementation: The second variant utilizes Locality Preserving Projection (LPP), an unsupervised approach that integrates both local manifold structure and spatial information. The weight matrix construction follows:

$$\omega_{ij} = \begin{cases} \exp\left(\frac{-\|x_i - x_j\|^2}{t}\right), & if\ x_i\ and\ x_j\ are\ neighbours\ of\ each\ other \\ 0, & otherwise \end{cases} \tag{6}$$

where:

- t is the heat kernel parameter
- Neighborhood relationship is defined by geometric proximity
- The exponential term preserves local manifold structure

4. Experiments

4.1. Experimental Setup

To rigorously evaluate the effectiveness of our proposed methods (LPNF-PCA and LPNF-LPP), we conducted comprehensive experiments using a diverse set of benchmark images under various noise conditions.

Experimental Setup:

1) Test Images: Four widely-used benchmark images (Fig 2):

- Cameraman
- Peppers
- Barbara
- Goldhill

Fig. 2. From left to right, the images are Cameraman, Peppers, Barbara, and Goldhill

2) Noise Scenarios:
- Gaussian noise contamination
- Mixed noise contamination

3) Comparative Methods:
Classical Approaches:
-Mean filter
-Median filter
-Bilateral filter
Advanced Techniques:
-Robust Principal Component Analysis (RPCA)
-Weighted Schatten p-norm Minimization (WSNM)

4)Performance Metrics:
Quantitative Evaluation:
Peak Signal-to-Noise Ratio (PSNR)
-Measures overall reconstruction quality
-Evaluates pixel-level accuracy

Structural Similarity Index (SSIM)
-Assesses structural preservation
-Quantifies perceptual quality

Normalized Mean Square Error (NMSE)
-Provides normalized error measurement
-Enables cross-image comparison

Qualitative Assessment:
-Visual comparison of restored images
-Analysis of detail preservation
-Evaluation of artifact suppression

4.2. Experimental Results and Analysis

First, we evaluate the performance of our proposed denoising methods using the Cameraman and Peppers images contaminated with zero-mean Gaussian noise at two different variance levels (0.2 and 0.3). The comprehensive denoising results for both images across different methods are presented in Tables 1 through 4.

Analysis of the Cameraman image results (Tables 1 and 2) demonstrates that our proposed methods achieve superior performance compared to competing approaches across nearly all evaluation metrics and scenarios. Specifically, both LPNF-PCA and LPNF-LPP show significant improvements over traditional filtering approaches such as mean, median, and bilateral filters. The quantitative gains are substantial, with minimum improvements of 0.04 in NMSE, 1.35 dB in PSNR, and 0.09 in SSIM. These consistent improvements across multiple metrics indicate the robust performance of our proposed methods in handling Gaussian noise at different intensity levels.

For the Peppers image (Tables 3 and 4), the LPNF-LPP variant demonstrates particularly impressive performance across both noise variance levels (0.2 and 0.3). The method maintains its effectiveness even at higher noise intensity, showcasing its robustness and stability in challenging denoising scenarios. The superior performance is consistent across all evaluation metrics, indicating that our method successfully preserves image structure while effectively removing noise. This comprehensive performance improvement over existing methods validates the effectiveness of our proposed approach in handling various types of image content and noise levels.

In summary, both LPNF-PCA and LPNF-LPP demonstrate clear advantages over existing methods across all three evaluation metrics (NMSE, PSNR, and SSIM). These consistent improvements across different images and noise levels validate the effectiveness and robustness of our proposed framework in image denoising applications.

Table 1. Performance comparison of different methods on the Cameraman polluted by Gaussian noise with variance of 0.2

Methods	NMSE	PSNR	SSIM
RPCA	0.1563±0.0006	13.64±0.02	0.3971±0.0027
WSNM	0.1733±0.0005	13.20±0.01	0.2930±0.0001
Mean filter	0.1606±0.0004	13.53±0.01	0.4893±0.0011
Median filter	0.1614±0.0006	13.50±0.02	0.3449±0.0013
Bilateral filter	0.1736±0.0004	13.19±0.01	0.2933±0.0012
LPNF-PCA	0.1147±0.0014	14.99±0.06	0.5805±0.0022
LPNF-LPP	0.1142±0.0038	15.02±0.14	0.5812±0.0024

To further validate the effectiveness of our proposed methods, we conducted a comprehensive evaluation using Barbara and Goldhill images contaminated with mixed noise conditions. The noise model combines zero-mean Gaussian noise (variance = 0.3) with Salt-and-Pepper noise (density = 0.2), representing a more challenging and realistic denoising scenario.

The experimental results for the Barbara image (Table 5) demonstrate the superior performance of our proposed methods compared to other state-of-the-art approaches.

Table 2. Performance comparison of different methods on the Cameraman polluted by Gaussian noise with variance of 0.3

Methods	NMSE	PSNR	SSIM
RPCA	0.2749±0.0004	11.19±0.01	0.3994±0.0041
WSNM	0.3245±0.0008	10.47±0.01	0.3019±0.0013
Mean filter	0.3053±0.0009	10.74±0.01	0.4852±0.0017
Median filter	0.3242±0.0010	10.47±0.01	0.3584±0.0014
Bilateral filter	0.3244±0.0010	10.47±0.01	0.3018±0.0010
LPNF-PCA	0.2113±0.0014	12.33±0.03	0.5653±0.0016
LPNF-LPP	0.2111±0.0021	12.34±0.04	0.5655±0.0020

Table 3. Performance comparison of different methods on the Peppers polluted by Gaussian noise with variance of 0.2

Methods	NMSE	PSNR	SSIM
RPCA	0.2001±0.0002	13.61±0.00	0.3148±0.0010
WSNM	0.2267±0.0002	13.07±0.00	0.2163±0.0004
Mean filter	0.1830±0.0002	14.00±0.00	0.6201±0.0010
Median filter	0.2013±0.0002	13.58±0.00	0.3305±0.0009
Bilateral filter	0.2213±0.0004	13.17±0.01	0.2430±0.0007
LPNF-PCA	0.1213±0.0019	15.78±0.07	0.6703±0.0018
LPNF-LPP	0.1200±0.0017	15.83±0.06	0.6710±0.0014

Both LPNF-PCA and LPNF-LPP achieve significant quantitative improvements, with notable gains of approximately 0.18 in NMSE and 4.32 dB in PSNR compared to competing methods. These substantial improvements indicate the robust capability of our methods in handling complex mixed noise scenarios while preserving important image details.

Similarly, the results for the Goldhill image (Table 6) corroborate these findings, showing consistent performance improvements across all evaluation metrics. The ability of our methods to maintain superior performance across different image content and mixed noise conditions demonstrates their robustness and general applicability.

In summary, both LPNF-PCA and LPNF-LPP consistently outperform existing comparative methods when applied to Barbara and Goldhill images contaminated with mixed noise. This superior performance in challenging mixed noise scenarios further validates the effectiveness of our proposed framework in real-world denoising applications.

Table 4. Performance comparison of different methods on the Peppers polluted by Gaussian noise with variance of 0.3

Methods	NMSE	PSNR	SSIM
RPCA	0.3945±0.0003	10.66±0.00	0.4396±0.0014
WSNM	0.4225±0.0002	10.36±0.00	0.2105±0.0006
Mean filter	0.3877±0.0004	10.74±0.00	0.5712±0.0007
Median filter	0.4126±0.0003	10.47±0.00	0.3213±0.0008
Bilateral filter	0.4244±0.0003	10.34±0.00	0.2447±0.0006
LPNF-PCA	0.2286±0.0019	13.03±0.04	0.6317±0.0012
LPNF-LPP	0.2255±0.0027	13.09±0.05	0.6334±0.0014

Table 5. Performance comparison of different methods on the Barbara with mixed noise

Methods	NMSE	PSNR	SSIM
RPCA	0.4095±0.0004	10.29±0.01	0.2634±0.0008
WSNM	0.5767±0.0006	8.80±0.01	0.0953±0.0007
Mean filter	0.2908±0.0008	11.77±0.01	0.3763±0.0020
Median filter	0.4522±0.0006	9.85±0.01	0.2304±0.0017
Bilateral filter	0.5770±0.0004	8.80±0.00	0.0952±0.0009
LPNF-PCA	0.1035±0.0040	16.26±0.16	0.3796±0.0015
LPNF-LPP	0.1077±0.0023	16.09±0.09	0.3815±0.0012

Table 6. Performance comparison of different methods on the Goldhill with mixed noise

Methods	NMSE	PSNR	SSIM
RPCA	0.3867±0.0007	10.49±0.01	0.2775±0.0015
WSNM	0.5659±0.0007	8.84±0.01	0.0654±0.0005
Mean filter	0.2806±0.0009	11.89±0.01	0.3936±0.0020
Median filter	0.4371±0.0005	9.96±0.01	0.1881±0.0020
Bilateral filter	0.5661±0.0007	8.84±0.01	0.0651±0.0007
LPNF-PCA	0.0880±0.0074	16.93±0.36	0.4035±0.0015
LPNF-LPP	0.0887±0.0060	16.90±0.31	0.4042±0.0024

Examining the qualitative results presented in Figure 3, our proposed methods demonstrate superior visual performance compared to existing denoising approaches when applied to images contaminated with zero-mean Gaussian noise (variance = 0.2). While established methods such as WSNM, median filter, and bilateral filter show significant residual noise in their recovered images, both LPNF-PCA and LPNF-LPP achieve more effective noise suppression while maintaining image fidelity.

The visual superiority of our methods is particularly evident in their ability to preserve crucial image details while effectively removing noise artifacts. Both LPNF-PCA and LPNF-LPP excel at retaining facial features and fine structural details of the original image, achieving a better balance between noise reduction and detail preservation. The recovered images show enhanced edge sharpness and more natural texture reproduction compared to the results from competing methods.

These qualitative improvements are characterized by clearer facial feature definition, better preservation of subtle texture details, and more balanced noise reduction without over-smoothing artifacts. The results maintain the natural contrast and overall visual characteristics of the original image while successfully eliminating noise contamination. These visual outcomes strongly complement our quantitative findings, demonstrating that our proposed methods not only achieve superior numerical metrics but also produce more visually appealing and faithful image reconstructions.

Figure 4 presents a comprehensive visual comparison of various denoising methods applied to the Barbara image contaminated with mixed noise (Gaussian noise with variance 0.3 and salt-and-pepper noise with density 0.2). The traditional filtering approaches demonstrate significant limitations in handling this complex noise scenario. Specifically, the mean filter tends to blur important image details while only partially removing noise. The median filter, while effective against salt-and-pepper noise, struggles to address the

Fig. 3. Visual comparison of different denoising methods on the Cameraman with Gaussian noise (variance is 0.2). From left to right and top to bottom, the images are the Original image, Noisy image, and the denoised images obtained by RPCA, WSNM, Mean filter, Median filter, Bilateral filter, LPNF-PCA, and LPNF-LPP, respectively

Fig. 4. Visual comparison of different denoising methods on the Barbara with mixed noise. From left to right and top to bottom, the images are the Original image, Noisy image, and the denoised images obtained by RPCA, WSNM, Mean filter, Median filter, Bilateral filter, LPNF-PCA, and LPNF-LPP, respectively

Gaussian noise component, resulting in loss of fine texture details. The bilateral filter preserves edges but fails to adequately remove the mixed noise, particularly in regions with complex textures.

In contrast, our proposed methods (LPNF-PCA and LPNF-LPP) demonstrate superior denoising performance in several aspects:

- Better preservation of fine texture details, particularly visible in the fabric patterns
- More effective removal of both Gaussian and salt-and-pepper noise components
- Improved edge preservation and structural integrity
- Enhanced visual clarity without introducing significant artifacts

– Better maintenance of the original image contrast and brightness

This visual comparison clearly demonstrates the advantages of our proposed methods in handling complex mixed noise scenarios while preserving important image details and structures.

5. Conclusions

In this study, we present a novel linear projection-based noise filtering (LPNF) framework for image denoising. The framework is innovatively constructed from the perspective of linear projection learning and demonstrates the ability to comprehensively utilize multiple structural information, including local spatial information, local manifold structure, and global structure, through the construction of diverse criteria for linear projection learning. Within this framework, two specialized implementations (i.e., LPNF-PCA and LPNF-LPP) were developed by incorporating the projection learning objective functions of Principal Component Analysis (PCA) and Locality Preserving Projection (LPP), respectively. Extensive experimental evaluations conducted on four standard test images with various noise types demonstrate that the proposed methods consistently outperform several state-of-the-art denoising approaches in terms of both quantitative metrics and visual quality. The superior performance validates the effectiveness and robustness of our proposed framework in image denoising applications.

Acknowledgments. This work was supported in part by the Hunan Provincial Key Research and Development Program under Grant 2023NK2011 and in part by the Hunan Provincial Natural Science Foundation of China under Grant 2022JJ40189.

References

1. Aswathy, C., Sowmya, V., Soman, K.: Hyperspectral image denoising using low pass sparse banded filter matrix for improved sparsity based classification. Procedia Computer Science 58, 26–33 (2015)
2. Gao, Z., Gu, C., Yang, J., Gao, S., Zhong, Y.: Random weighting-based nonlinear gaussian filtering. IEEE Access 8, 19590–19605 (2020)
3. Gholami Bahador, F., Mokhtary, P., Lakestani, M.: Mixed poisson-gaussian noise reduction using a time-space fractional differential equations. Information Sciences 647, 119417 (2023)
4. Gonzalez, R.C., Woods, R.E.: Digital Image Processing (3rd Edition). Pearson Education (2008)
5. Goyal, B., Dogra, A., Agrawal, S., Sohi, B.S., Sharma, A.: Image denoising review: From classical to state-of-the-art approaches. Information fusion 55, 220–244 (2020)
6. He, L., Zhang, Q., Yang, X., Wang, Y., Wang, C.: Sln-red: Regularization by simultaneous local and nonlocal denoising for image restoration. IEEE Signal Processing Letters (2023)
7. Hotelling, H.: Analysis of a complex of statistical variables into principal components. Journal of Educational Psychology 24(6), 417–441 (1933)
8. Huang, J., Jin, Z.: Enhanced image denoising with diffusion probability and dictionary learning adaptation. Technical gazette 31(3), 774–783 (2024)
9. Huang, T.S., Yang, G.J., Tang, G.Y.: A fast two-dimensional median filtering algorithm. IEEE Transactions on Acoustics, Speech, and Signal Processing 27(1), 13–18 (1997)

10. Jebur, R.S., Der, C.S., Hammood, D.A., Weng, L.Y.: Image denoising techniques: An overview. AIP Conference Proceedings 2804(1), 020002 (09 2023)
11. Jolliffe, I.T.: Principal Component Analysis (2nd Edition). Springer (2002)
12. Liu, J., Sun, H., Wu, M., Yang, J.: Gpu implementation of a fast multichannel wiener filter algorithm for active noise control. IEEE Signal Processing Letters (2024)
13. Mafi, M., Martin, H., Cabrerizo, M., Andrian, J., Barreto, A., Adjouadi, M.: A comprehensive survey on impulse and gaussian denoising filters for digital images. Signal Processing 157, 236–260 (2019)
14. Pearson, K.: On lines and planes of closest fit to systems of points in space. Philosophical Magazine 2(11), 559–572 (1901)
15. Saadia, A., Rashdi, A.: A speckle noise removal method. Circuits, Systems, and Signal Processing 37, 2639–2650 (2018)
16. Schölkopf, B., Smola, A., Müller, K.R.: Nonlinear component analysis as a kernel eigenvalue problem. Neural Computation 10(5), 1299–1319 (1997)
17. Selesnick, I.W., Graber, H.L., Pfeil, D.S., Barbour, R.L.: Simultaneous low-pass filtering and total variation denoising. IEEE Transactions on Signal Processing 62(5), 1109–1124 (2014)
18. Susladkar, O., Deshmukh, G., Nag, S., Mantravadi, A., Makwana, D., Ravichandran, S., Chavhan, G.H., Mohan, C.K., Mittal, S., et al.: Clarifynet: A high-pass and low-pass filtering based cnn for single image dehazing. Journal of systems architecture 132, 102736 (2022)
19. Tang, J., Wang, Y., Cao, W., Yang, J.: Improved adaptive median filtering for structured light image denoising. In: 2019 7th International conference on information, communication and networks (ICICN). pp. 146–149. IEEE (2019)
20. Thanh, D., Surya, P., et al.: A review on ct and x-ray images denoising methods. Informatica 43(2) (2019)
21. Thanh, D.N., Hien, N.N., Kalavathi, P., Prasath, V.S.: Adaptive switching weight mean filter for salt and pepper image denoising. Procedia Computer Science 171, 292–301 (2020)
22. Tomasi, C., Manduchi, R.: Bilateral filtering for gray and color images. In: Proceedings of the Sixth International Conference on Computer Vision (ICCV). pp. 839–846. IEEE, Bombay, India (1998)
23. Uddin, M.P., Mamun, M.A., Hossain, M.A.: Pca-based feature reduction for hyperspectral remote sensing image classification. IETE Technical Review 38(4), 377–396 (2021)
24. Wang, J., Wu, Y., Li, B., Yang, Z., Nie, F.: Fast anchor graph preserving projections. Pattern Recognition 146, 109996 (2024)
25. Yang, R., Li, D.: Adaptive wavelet transform based on artificial fish swarm optimization and fuzzy c-means method for noisy image segmentation. Computer Science and Information Systems 19(3), 1389–1408 (2022)
26. Zhang, J., Li, Z.y., Wang, L.z., Chen, Y.p.: Salt-and-pepper denoising method for colour images based on tensor low-rank prior and implicit regularization. IET Image Processing 17(3), 886–900 (2023)
27. Zhang, X.: Center pixel weight based on wiener filter for non-local means image denoising. Optik 244, 167557 (2021)
28. Zhang, X., Liao, H., Du, X., Xu, B.: A fast hybrid noise filtering algorithm based on median-mean. In: 2018 IEEE International Conference on Mechatronics and Automation (ICMA). pp. 2120–2125. IEEE (2018)

Congyin Cao received the B.S. degree in software engineering from Zhongyuan University of Technology, Zhengzhou, China, in 2022. He is currently working toward the M.Agr. degree in agricultural engineering and information technology with the College

of Information and Intelligence, Hunan Agricultural University, Changsha, China. His research interests include remote sensing image processing and analysis field, especially remote sensing image feature extraction and classification technology.

Yangjun Deng received the Ph.D. degree in signal and information processing from the School of Information Science and Technology, Southwest Jiaotong University, Chengdu, China, in 2020. From 2018 to 2019, he was a Visiting Scholar along with Prof. Qian Du at Mississippi State University, Starkville, MS, USA, to study on the dimensionality reduction of hyperspectral images. He is currently a associate professor with the College of Information and Intelligence, Hunan Agricultural University, Changsha, China. His research interests include pattern recognition, remote sensing image processing, and agricultural information processing.

Menglong Yang received the B.S. degree in computer science and technology and M.Agr. degree in agricultural engineering and information technology from Hunan Agricultural University, Changsha, China, in 2021 and 2024, respectively. He is currently pursuing the Ph.D. degree in forestry engineering with the School of Central South University of Forestry and Technology. His research interests include machine learning and pattern recognition.

Xinghui Zhu received the M.S. degree in computer science and technology from National University of Defense Technology, Changsha, China, in 2004. He received the Ph.D. degree in land resources and information technology from Hunan Agricultural University, Changsha, China, in 2018. From 2016 to 2023, he served as dean with the College of Information and Intelligence, Hunan Agricultural University, Changsha, China. He is currently a member of the National Steering Committee of Agricultural Graduate Education, vice chairman of Hunan Provincial Computer Specialized Committee, and executive director of Hunan Computer Federation. His research interests include Artificial Intelligence, Big Data, Smart Agriculture, etc. He has already won one first prize of Hunan Provincial Scientific and Technological Progress in related fields, and has presided over four national projects such as the National Science and Technology Support Program and the National Key Research and Development Program, as well as eight provincial and ministerial projects such as the Hunan Provincial Natural Science Foundation and the Hunan Provincial Key Research and Development Program. He has more than 60 publications in these areas.

Received: November 07, 2024; Accepted: December 17, 2024.